

Contribution to Experiments of a Free Surface Supercritical Flow over an Uneven Bottom

M. Bougamouza, M. Bouhadef, T. Zitoun

Abstract—The aim of this study is to examine, through experimentation in the laboratory, the supercritical flow in the presence of an obstacle in a rectangular channel. The supercritical regime in the whole hydraulic channel is achieved by adding a convergent. We will observe the influence of the obstacle shape and dimension on the characteristics of the supercritical flow, mainly the free-surface elevation and the velocity profile. The velocity measurements have been conducted with the one dimension laser anemometry technique.

Keywords—Experiments, free-surface flow, hydraulic channel, uneven bottom, laser anemometry, supercritical regime.

I. INTRODUCTION

THE study of supercritical flow in a horizontal rectangular channel, with an obstacle placed on the bottom, was conducted by different authors and in different ways. The literature in this field is quite abundant, whether numerically or experimentally.

Besides [1], one can note, among others, [2]-[10] to name a few of them. An experimental study [11] showed good qualitative agreement of the experimental free-surface and that deduced theoretically, including the horizontal component velocity profiles. In a mathematical study, [12] showed that the flow of a fluid in a channel with an obstacle lying on a flat bottom generates a free-surface which is no longer horizontal. In the case of the supercritical flow, if the obstacle is not too high, there is unique solution. Bukreev [2] gave a representation of the dimensionless free-surface profiles above obstacles of different shapes and different dimensions. Bouhadef [5] shows, in the case of a supercritical regime, through a comparative study with the results given by [13] and [14], the results of the free surface are consistent even for configurations strongly not linear. Liapidevskii et al. [8] proposed mathematical models for nonlinear solutions for supercritical flow over a semi spherical obstacle.

II. EXPERIMENTATION

A. Description

The experimental study is conducted in the case of a hydraulic channel flow which regime is supercritical upstream of the lying obstacle. To get such a configuration, we have added a convergent (nozzle) at the entrance. It has been

introduced to reduce the cross section of flow to a narrowed outlet opening $H = 2.5$ cm, thus allowing to increase the velocity entrance (see [15]).

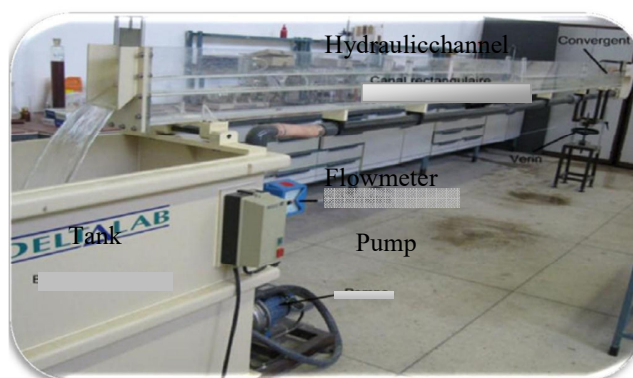


Fig. 1 View of the hydraulic channel



Fig. 2 Level gauge

Our experiments were carried out in a rectangular channel with variable slope, which we disposed horizontally.

The channel has a width $b = 75$ mm and a length $l = 6$ m; it is made of transparent Plexiglas which allows complete visualization of the flow. It is assembled by means of a special assembly which ensures parallel walls with a height of 160 mm. The perfect rigidity of the channel is provided by a Plexiglas box girder. The water supply is provided in a closed circuit by a horizontal axis pump. Flow control is achieved by a manual valve that allows us to vary the discharge Q from 1.6 m³/h to 16 m³/h.

To determine the Froude number, we use the upstream average velocity U which is given by the discharge $Q = UbH$. We have previously calibrated the flowmeter and the

M. Bouhadef and T. Zitoun are with the LEGHYD Laboratory, Faculty of Civil Engineering, University of Sciences and Technology Houari Boumediene (USTHB), BP 32, Bab-Ezzouar, Algiers, Algeria (e-mail: mbouhadef@usthb.dz).

M. Bougamouza has prepared a Magister in the LEGHYD Laboratory.

relationship between the real flow rate and the indicated one is given by:

$$Q = 1.0522Q_r - 0.0001$$

Q_r (m^3/s) is the value read on the flowmeter and Q the effective discharge.

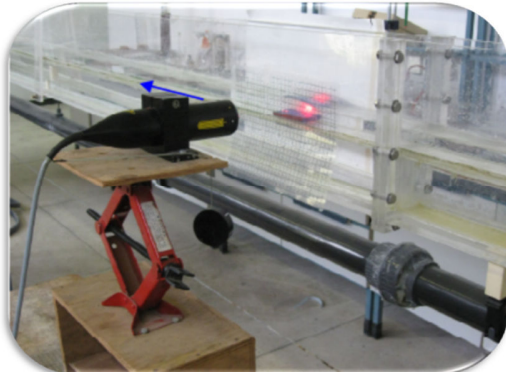


Fig. 3 Laser Döppler Anemometer

Several types of obstacles, with a width $b=7.5$ cm, and different profiles and length sizes, are used. The first obstacle has a rectangular shape (different heights) and has a length of 8cm. The obstacle 2 has a trapezoidal shape, its height is $s=7$ mm and a length $l=8$ cm. The barrier 3 has a symmetric triangular shape, its height is $s=7$ mm and a length $l=8$ cm. A peak level meter (Fig. 2) is used to measure water levels in the channel. The laser anemometer (Fig. 3), which is one of the most used in basic and applied research in fluid mechanics, is used to measure the velocity at each point of the water flow.

B. Results and Discussion

The experimental obtained results show that the effects of an obstacle, on the supercritical flow regime, primarily depends on its profile and the dimensionless parameter $S =$

$$\frac{s}{H} \text{ and the Froude number } Fr = \frac{Q}{bH\sqrt{gH}}.$$

1. Free-Surface Profile

Using a level gauge, the free-surface heights over the three obstacles were measured. For $s=1$ cm, the results are shown in Figs. 4-7 where X is the dimensionless abscissa ($\frac{x}{H}$) and Y the dimensionless level ($\frac{y}{H}$).

Fig. 4 shows that the profile of the free-surface is asymmetrical relative to the center of the obstacle. We note some sudden elevation in the first interaction of the flow with the vertical face of the obstacle (for $x=0$). This increase peaked at the interval of ($0.4 \leq X \leq 0.8, Y=1.5$).

Fig. 5 shows that the free-surface, above the trapezoidal step, has a symmetrical hump shape, its maximum height being lower compared to that obtained for the rectangular obstacle; this increase peaked at the point ($x=1.2, Y=1.36$).

Fig. 6 shows that the free-surface profile, above the triangular barrier, has the shape of a symmetrical bump relative to the center of the obstacle. The elevation is lower compared to the two previous cases.

For the trapezoidal and triangular obstacles, the free-surface profiles are symmetrical relative to the obstacle. For the rectangular step, it appears a sudden free-surface elevation upstream of the obstacle; this is due to the obstacle geometry which causes an asymmetry in the free-surface shape. One must also note a difference in the water level upstream and downstream of all obstacles.

Fig. 7 shows the free-surface elevations above the rectangular step, for different heights ($S=0.2, S=0.28, S=0.36$ and $S=0.44$). As indicated in Fig. 1, the profile shape is asymmetric. It can be noted that the free-surface elevation increases with the obstacle's height.

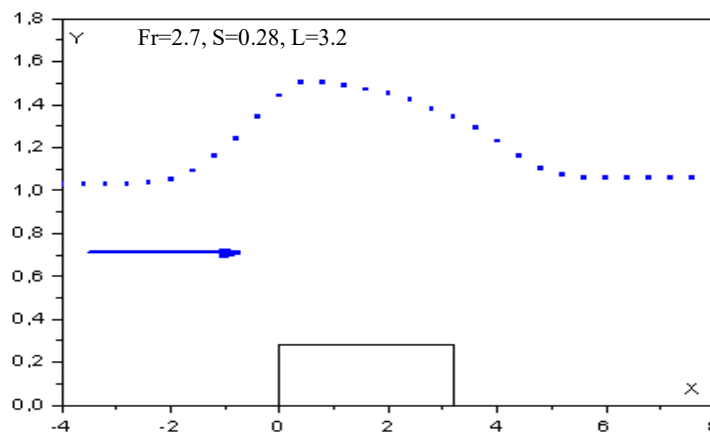


Fig. 4 Free-surface profile above the rectangular step

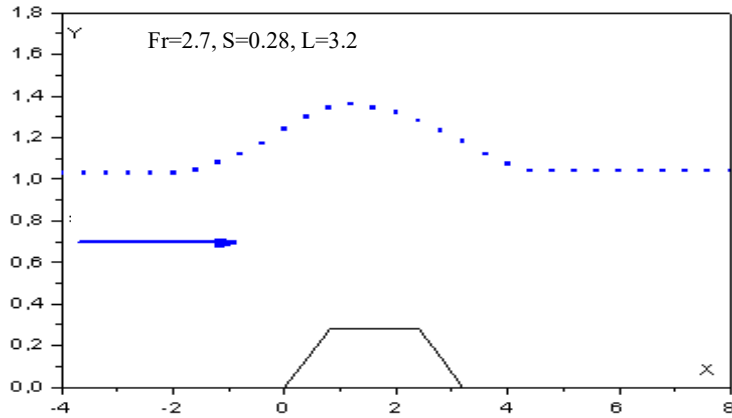


Fig. 5 Free-surface profile above the trapezoidal step

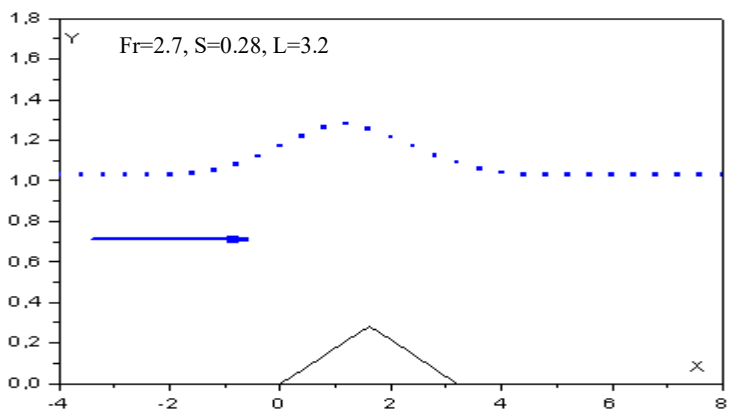


Fig. 6 Free-surface profile above the triangular step

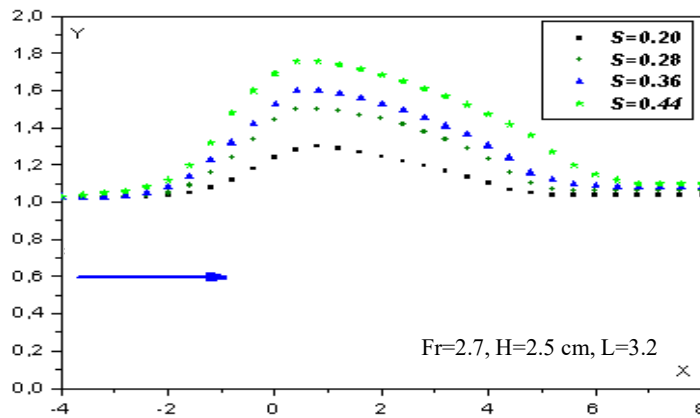


Fig. 7 Profiles above the rectangular step for various heights

Fig. 8 shows the free-surface profiles above the rectangular step for different Froude numbers. The highest points of each bump change their coordinates with the Froude number. For $Fr = 2.7$, the highest point is $(X = 0.4, Y = 1.5)$; for $Fr = 3.04$ $(X = 0.8, Y = 1.49)$ and for $Fr = 4.3$ $(X = 1.6, Y = 1.41)$. It can be therefore noted that the Froude number increasing involves a lowering of the bump's height and the free-surface profile tends to become symmetrical ($Fr=4.3$).

2. Velocity Profiles

The velocity is measured using a Laser Döppler

Anemometer. The longitudinal component velocity profiles (u) are then given in dimensionless values where $u_0 = \frac{Q}{bH}$ is the mean velocity.

Fig. 9 shows the velocity profiles upstream and downstream of the steps. One can note that the downstream profiles obtained, for the rectangular step, have relatively low values relative to those of the trapezoidal and triangular obstacles; this is due to the energy's loss when crossing the obstacles.

According to Figs. 9 and 10, it can be noted that the step's

shape has a great importance in the velocity profile evolution.

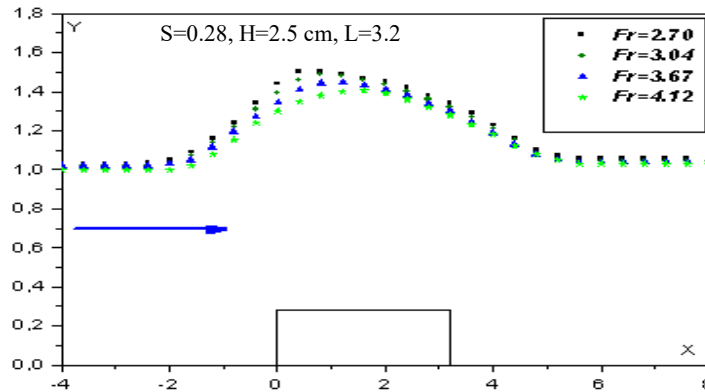


Fig. 8 Free-surface for different Froude numbers (rectangular step)

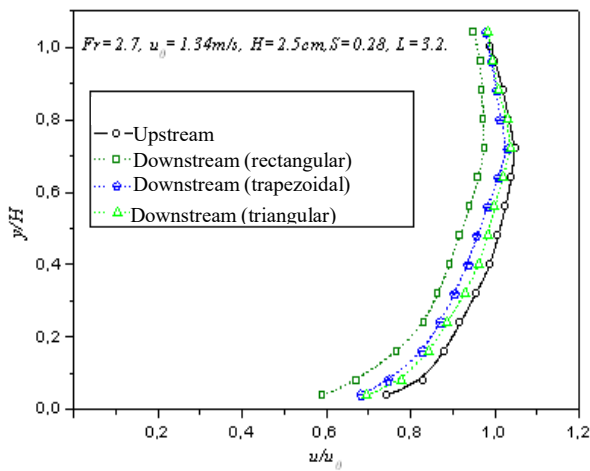


Fig. 9 Velocity profiles upstream and downstream for different steps

Fig. 10 shows the above obstacles velocity profiles. At the top of the obstacle, the velocity values are lower for rectangular and trapezoidal obstacles compared with the triangular one. The water streamlines upstream the triangular step are not very bothered by the obstacle rather than the other two obstacles. After this, the velocities increase and reach their maximum at almost half the water depth.

Fig. 11 shows that for large values of the Froude number, the energy loss between the upstream and downstream is important; for low Froude number values, this decrease is relatively low.

III. CONCLUSION

As it was already mentioned by [16], one shows, through this experimental study carried out in a hydraulic channel, that the torrential mode can be easily established by adding a convergent at the entry of the channel. Thus, by choosing an adequate height H at the exit of the canal, we can reach high Froude number values.

It can be suggested that downstream of a dam and to dissipate more energy due to the flood, one could introduce an obstacle with an adequate shape before creating a hydraulic jump.

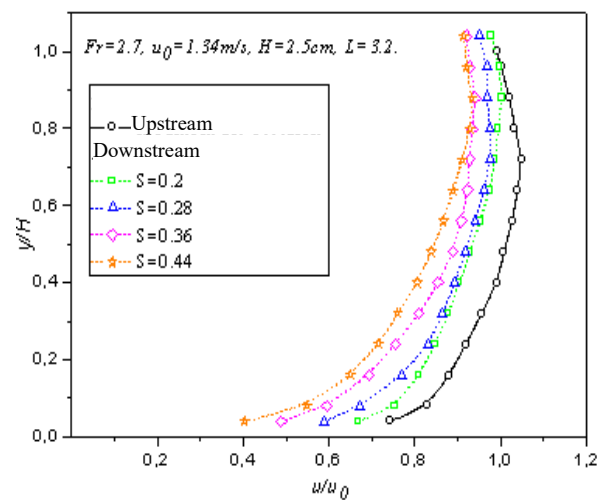


Fig. 10 Velocity profiles upstream and downstream of the rectangular step for various heights

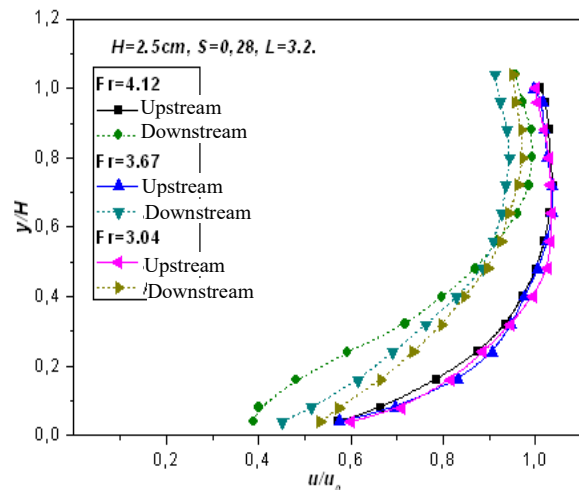


Fig. 11 Velocity profiles upstream and downstream of a rectangular step for different Froude numbers

ACKNOWLEDGMENT

The authors would like to thank the DGRSDT (Algeria) for

its financial support to the LEGHYD laboratory.

REFERENCES

- [1] Lamb H., 1945, Hydrodynamics, 6th ed. Dover, New York.
- [2] Bukreev V. I., 2002, Supercritical flow over a sill in an open channel, Journal of Applied Mechanics and Technical Physics, Vol. 43, No. 6, pp. 830, 835.
- [3] Ghaleb A.F., Hefni A.Z., 1987, Wave free, two-dimensional gravity flow of an inviscid fluid over a bump. J. Mec. Theor. Appl., 6, 4.
- [4] King A.C., Bloor M.T.G., 1987, A free surface flow over a step. J. Fluid. Mech. 182, 193-208.
- [5] BouhadeF M., 1988, Contribution à l'étude des ondes de surface dans un canal hydraulique. Application à l'écoulement au-dessus d'un obstacle immergé. Thèse de Doctorat-ès-Sciences, U.E.R. C. E. A. T., Poitiers (France).
- [6] Boutros Y.Z., Abdelmalek M.B. and Massoud S.Z., 1986, Linearized solution of a flow over a non uniform bottom, J. of Comput and Appli. Math., 16, 105-116.
- [7] Bouzelha-Hammoum K, BouhadeF M, Zitoun T, 2006, Numerical study of 2D free-surface waveless flow over a bump, WSEAS Transactions on Fluid Mechanics, Issue 6, Vol. 1, 732-737.
- [8] Liapidevskii V. Y. and Xu Z., 2006, Breaking of waves of limiting amplitude over an obstacle, Journal of Applied Mechanics and Technical Physics, Vol. 47, No. 3, pp. 307-313.
- [9] Bouinoun M., BouhadeF M., Zitoun T., 2012, Free surface flow over an uneven bottom: Experiments in a hydraulic channel, International Conference on Metallurgical, Manufacturing and Mechanical Engineering, Dubai, UAE.
- [10] Lustrì C.-J., Mccue S.-W. and Binder B.-J., 2012, Free surface flow past topography: beyond-all-orders approach. European Journal of Applied Mathematics, Vol. 23, Issue 04, 441-467.
- [11] Bouzelha-Hammoum K, BouhadeF M, Zitoun T & Guendouzen T, 2008, Contribution to the study of a free-surface supercritical flow above an obstacle: theory and laboratory work, 6th IASME/WSEAS International Conference on Fluid Mechanics and Aerodynamics.
- [12] Teniou D., 2007, Sur l'écoulement d'un fluide dans un canal avec obstacle au fond, Annales mathématiques Blaise Pascal, Volume 14, n°2, 255-265.
- [13] Forbes L. K., Schwartz L. W., 1982, Free-surface flow over a semicircular obstruction. J.Fluid Mech., 114, 299, 314.
- [14] Cahouet J., Lenoir M.. 1983, Résolution numérique du problème non linéaire de la résistance de vagues bidimensionnelle. C.R.Acad. Sci. de Paris. 297.
- [15] Bouinoun M., BouhadeF M., 2015, Experiments of a free-surface flow in a hydraulic channel over an uneven bottom, International Journal of Civil, Environmental, Structural, Construction and Architectural Engineering, Vol. 7, n°9, 694-698.
- [16] Bougamouza A., Guendouzen-Dabouz T., Bouzelha-Hammoum K., BouhadeF M. & Zitoun T., 2010, 2D supercritical free-surface flow: an experimental study, HEFAT 2010, Antalya.